

Multivariable Control of Smart Timoshenko Beam Structures Using POF Technique

T.C. Manjunath¹, *Student Member IEEE*, B. Bandyopadhyay², *member IEEE*

Abstract—Active Vibration Control (AVC) is an important problem in structures. One of the ways to tackle this problem is to make the structure smart, adaptive and self-controlling. The objective of active vibration control is to reduce the vibration of a system by automatic modification of the system's structural response. This paper features the modeling and design of a Periodic Output Feedback (POF) control technique for the active vibration control of a flexible Timoshenko cantilever beam for a multivariable case with 2 inputs and 2 outputs by retaining the first 2 dominant vibratory modes using the smart structure concept. The entire structure is modeled in state space form using the concept of piezoelectric theory, Timoshenko beam theory, Finite Element Method (FEM) and the state space techniques. Simulations are performed in MATLAB. The effect of placing the sensor / actuator at 2 finite element locations along the length of the beam is observed. The open loop responses, closed loop responses and the tip displacements with and without the controller are obtained and the performance of the smart system is evaluated for active vibration control.

Keywords—Smart structure, Timoshenko theory, Euler-Bernoulli theory, Periodic output feedback control, Finite Element Method, State space model, Vibration control, Multivariable system, Linear Matrix Inequality

I. INTRODUCTION

PIEZOELECTRIC materials are capable of altering the structure's response through sensing, actuation and control. Piezoelectric elements can be incorporated into a laminated composite structure, either by embedding it or by mounting it onto the surface of the host structure [10], [31]. Vibration control of any system is always a formidable challenge for any control system designer. Active control of vibrations relieves a designer from strengthening the structure from dynamic forces and the structure itself from extra weight and cost. The need for intelligent structures such as smart structures arises from the high performance requirements of

such structural members in numerous applications. Intelligent structures are those which incorporate actuators and sensors that are highly integrated into the structure and have structural functionality, as well as highly integrated control logic, signal conditioning and power amplification electronics [8].

A vibration control system consists of 4 parts, viz., actuator, controller, sensor and the system or the plant, which is to be controlled. When an external force f_{ext} is applied to the beam, it is subjected to vibrations. These vibrations should be suppressed quickly. Fully active actuators like the Piezoelectrics, MR Fluids, Piezoceramics, ER Fluids, Shape Memory Alloys, PVDF, etc., can be used to generate a secondary vibrational response in a mechanical system. This could reduce the overall response of the system plant by the destructive interference with the original response of the system, caused by the primary source of vibration [6], [8], [18], [21].

Feedback control of vibrations in mechanical flexible systems has numerous applications, like in aircrafts, active noise and shape control, acoustic control, earthquakes, control of space structures and in control of flexible manipulators. Active control of unwanted disturbance consists of canceling the disturbance by the deliberate addition of a second disturbance, equal in magnitude but opposite in direction. Applying forces whose magnitudes and phases are determined by a controller can control vibrations of single and multiple Degree Of Freedom (DOF) systems. The inputs to the controller are displacements or velocities measured at various points in the system.

Extensive research in modeling of piezoelectric materials in building actuators and sensors for structure is reported here. Investigations of Crawley and Luis [8] emphasized on the derivation of sensor / actuator modeling of piezo-electric materials. Moreover, the control analysis of cantilever beams using these sensors / actuators have been studied by Bailey and Hubbard [6]. Culshaw [10] gave a brief introduction to the concept of smart structure, its benefits and applications. Hanagud, *et al.*, [21] developed a Finite Element Model (FEM) for an active beam with many distributed piezoceramic sensors / actuators coupled by signal conditioning systems and applied optimal output feedback control. Fanson *et al.*, [18] performed some experiments on a beam with piezoelectrics using positive position feedback.

Hwang and Park [22] presented a FE model for piezoelectric sensors and actuators. Choi *et al.* [12] discussed

¹Mr. Tadaga Channaveerappa Manjunath is a Research Scholar (student member IEEE, IOP, SPIE and a life member of ISSS, SSI, ISTE) in the interdisciplinary Programme in Systems and Control Engineering, Indian Institute of Technology Bombay, Powai, Mumbai-400076, Maharashtra, India. (Corresponding author phone : +91 22 25780263 / 25767884 ; Fax: +91 22 25720057 ; E-mail: tcmanju@sc.iitb.ac.in, tcmanjunath@gmail.com, URL : <http://www.sc.iitb.ac.in/~tcmanju>).

²Dr. Bijnan Bandyopadhyay is with the Interdisciplinary Programme in Systems and Control Engineering, Indian Institute of Technology Bombay, IIT Bombay, Mumbai-76, Maharashtra, India and is currently in the Professor cadre. (Phone : +91 22 25767889 / Fax: +91 22 25720057 ; Email : bijnan@ee.iitb.ac.in, URL : <http://www.sc.iitb.ac.in/~bijnan>).

about the control techniques of flexible structures using distributed piezoelectric sensors / actuators. An effective vibration control scheme using periodic output feedback technique was presented by Manjunath and Bandyopadhyay in [26]. The effect of failure of one of the actuators in a multivariable smart system and its control using the periodic output feedback control law was discussed in [27] by Manjunath and Bandyopadhyay.

The outline of the paper is as follows. A brief review of related literature about the types of beam models is given in Section 2. Section 3 gives a brief introduction to the modeling technique (sensor / actuator model, finite element model, state space model) of the smart cantilever beam. A brief review of the controlling technique, viz., the periodic output feedback control technique and the design of the controller to control the first two modes of vibration of the system is discussed in Section 4. POF controller design is discussed in Section 5. Simulation results are presented in Section 6 followed by the concluding section, appendix, nomenclature and references.

II. REVIEW OF BEAM MODELS AND PIEZO ACTUATION

The study of physical systems such as beams frequently results in partial differential equations, which either cannot be solved analytically, or lack an exact analytic solution due to the complexity of the boundary conditions. For a realistic and detailed study, a numerical method must be used to solve the problem. The finite element method is often found the most adequate. Over the years, with the development of modern computers, the finite element method [34] has become one of the most important analysis tools in engineering. Basically, the finite element method consists of a piecewise application of classical variational methods to smaller and simpler sub domains called finite elements connected to each other in a finite number of points called nodes. A precise mathematical model is required for the controller design for vibration control to predict the structure's response. Two beam models in common use in the structural mechanics are the Euler-Bernoulli beam model and the Timoshenko beam model, which are considered here below.

A. Euler-Bernoulli Model

This model often called as the classical beam model accounts for the bending moment effects on stresses and deformations. The effect of transverse shear forces on beam deformation is neglected. Its fundamental assumption is that cross sections remain plane and normal to the deformed longitudinal axis before and after bending. This assumption is valid if length to thickness ratio is large and for small deflection of beam. However, if length to thickness ratio is small, the plane section will not remain normal to the neutral axis after bending and the total rotation θ will be due to the bending stress alone. This rotation occurs about a neutral axis that passes through the centroid of the cross section of the beam as shown in Fig. 1.

Crawley, *et al.* [8] have developed analytical models of beams with piezoelectric actuators. These models illustrate the

mechanics of Euler-Bernoulli beams with surface mounted actuators and the analytical results have been verified by carrying out experiments. In practical situations, a large number of modes of vibrations contribute to the structure's performance. Since the shear forces, axial displacement are neglected in *Euler-Bernoulli theory*, slightly inaccurate results may be obtained. *Timoshenko Beam Theory* is used to overcome the drawbacks of the Euler-Bernoulli beam theory by considering the effect of shear and axial displacements.

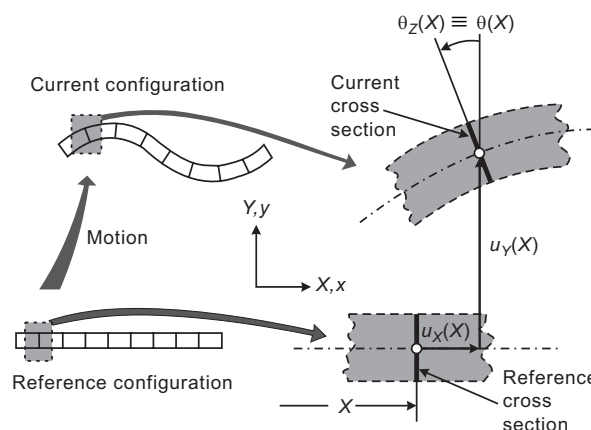


Fig. 1 Euler-Bernoulli beam model

B. Timoshenko model

This model corrects the classical beam model with first-order shear deformation effects. In this model, the cross sections of the beam remain plane and rotate about the same neutral axis as the Euler-Bernoulli model, but do not remain normal to the deformed longitudinal axis. The deviation from normality is produced by a transverse shear that is assumed to be constant over the cross section. Thus, the Timoshenko Beam model is superior to Euler-Bernoulli model in precisely predicting the beam response. The total slope of the beam in this model consists of two parts, one due to bending θ , and the other due to shear β . Chandrashekhara and Varadarajan [9] have presented a finite element model of a composite beam using a higher-order shear deformation theory. Piezoelectric elements have been used to produce a desired deflection in beams with Clamped-Free (C-F), Clamped-Clamped (C-C) and simply supported beams.

Aldraihem *et al.* [1] have developed a laminated beam model using two theories; namely, Euler-Bernoulli beam theory and Timoshenko beam theory. Here, the piezoelectric layers have been used to control the vibration in a cantilever beam. Donthireddy and Chandrashekhara [17] presented a new technique of modeling and shape control of composite beam with embedded piezoelectric actuators. A finite element model was designed for the dynamic analysis of Timoshenko beam by Thomas and Abbas [35]. Doschner and Enzmamam [16] presented a new type of controller for the vibrations of a Timoshenko beam. Closed form of solutions for the deflection control of laminated composite beams were presented by Abramovich [2]. In [25], Manjunath and

Bandyopadhyay discussed the vibration control of beams modeled using Timoshenko beam theory and using different aspect ratios of the beam.

Recently, shear piezoelectric actuators have been used to generate deflection and to reject vibration in beams. The idea of exploiting the shear mode to create transverse deflection in beams was first suggested by Sun and Zhang [32]. A finite element approach was used by Benjeddou, *et al.* [7] to model a beam with shear and embedded piezoelectric elements. The finite element model employed the displacement field of Zhang and Sun [40]. It was shown that the finite element results agree quite well with the analytical results. Raja, *et al.* [30] extended the finite element model of Benjeddou's research team to include a vibration control scheme. It was observed that the shear actuator is more efficient in rejecting vibration than without considering the shear for the same control effort.

Aldraihem and Khdeir [3] proposed analytical models and exact solutions for beams with shear piezoelectric actuators. The models are based on Timoshenko beam theory and Higher-Order Beam Theory (HOBT). Exact solutions were obtained by using the state-space approach. The deflections of beams with various boundary conditions were investigated. The effect of shear coefficient was discussed in the Timoshenko beam theory by Cooper [11]. Deflection analysis of the beam with extension and shear piezoelectric patches was reported by Ahmed and Osama [4]. An improved two-node Timoshenko beam model was presented by Friedman and Kosmatka [23] which is used in our work. Azulay *et al.* [5] have presented analytical formulation and closed form solutions of composite beams with piezoelectric actuators.

Timoshenko beam theory is used in the present work to generate the FE model [28] of a MIMO cantilever beam with surface mounted sensors and actuators as collocated pairs, i.e., one above and below the corresponding finite elements of the beam. Further, the periodic output feedback control design and its application to control the first two structural vibration modes of the smart flexible Timoshenko cantilever beam is considered.

III. MATHEMATICAL MODELING OF SMART BEAM

Few researchers have well established a mathematical finite element E-B model. These models do not consider the shear effects, axial effects, etc.,... Modeling of smart structures by shear deformable (Timoshenko) theory is limited. In our work, the effect of shear has been considered in modeling

Consider a aluminum cantilever beam as shown in Fig. 2 divided into 4 finite elements as shown in Fig. 3. The piezoelectric element is bonded on two discrete sections (two finite elements) of the surface of the beam as surface mounted sensor / actuator pairs. The piezoelectric element is obtained by sandwiching the regular beam element between two thin piezoelectric layers. The bottom layer is acting as a sensor and the top layer is acting as an actuator as shown in the Fig. 2.

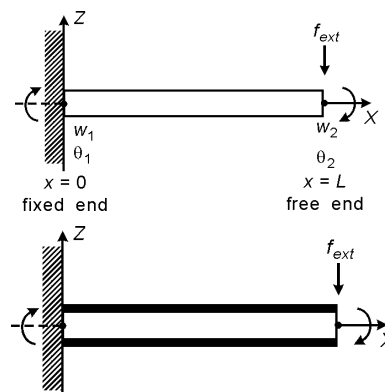


Fig. 2 A regular flexible beam and a smart Aluminum Timoshenko cantilever beam embedded with surface mounted

The element is assumed to have two structural DOF's (w, θ) at each nodal point and an electrical DOF : a transverse deflection and an angle of slope or rotation. Since the voltage is constant over the electrode, the number of DOF is one for each element. The electrical DOF is used as a sensor voltage or actuator voltage. Corresponding to the two DOF's, a bending moment acts at each nodal point, i.e., counteracting moments are induced by the piezoelectric patches. The bending moment resulting from the voltage applied to the actuator adds a positive finite element bending moment, which is the moment at node 1, while subtracting it at node 2.

In modeling of the smart beam, the following assumptions are made. The mass and stiffness of the adhesive used to bond the sensor / actuator pairs to the master structure is being neglected. The smart cantilever beam model is developed using 2 piezoelectric beam elements, which includes sensor and actuator dynamics and remaining beam elements as regular beam elements based on Timoshenko beam theory assumptions. The cable capacitance between the piezo patches and the signal-conditioning device is considered negligible and the temperature effects are neglected. The signal conditioning device gain is assumed as 100.

An external force input f_{ext} (impulse) is applied at the free end of the smart beam. The beam is subjected to vibrations and takes a lot of time for the vibrations to dampen out. These vibrations are suppressed quickly in no time by the closed loop action of the controller, sensor and actuator. Thus, there are two inputs to the plant. One is the external force input f_{ext} (impulse disturbance), which is taken as a load matrix of 1 unit in the simulation and the other input is the control input u to the actuator from the POF controller. The dimensions and properties of the aluminum cantilever beam and piezoelectric sensor / actuator used are given in Tables 1 and 2 respectively.

A. Finite Element Modeling of the regular beam element

A regular beam element is shown in Fig. 2. The longitudinal axis of the regular beam element lies along the X-axis. The element has constant moment of inertia, modulus of elasticity, mass density and length [5], [23], [41].

TABLE I
 PROPERTIES OF THE FLEXIBLE CANTILEVER BEAM ELEMENT

Parameter (with units)	Symbol	Numerical values
Length (m)	l_b	0.5
Width (m)	b	0.024
Thickness (mm)	t_b	1
Young's modulus (GPa)	E_b	193.06
Density (kg/m ³)	ρ_b	8030
Damping constants	α, β	0.001, 0.0001

TABLE II
 PROPERTIES OF THE PIEZO - SENSOR / ACTUATOR ELEMENT

Parameter (with units)	Symbol	Numerical values
Length (m)	l_p	0.125
Width (m)	b	0.024
Thickness (mm)	t_a, t_s	0.5
Young's modulus (GPa)	E_p	68
Density (kg/m ³)	ρ_p	7700
Piezo strain constant (m/V)	d_{31}	125×10^{-12}

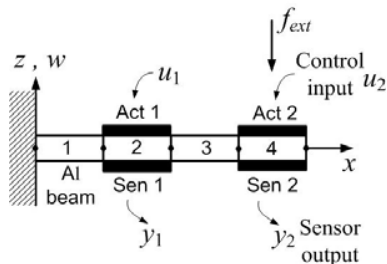


Fig. 3. A MIMO smart Timoshenko beam

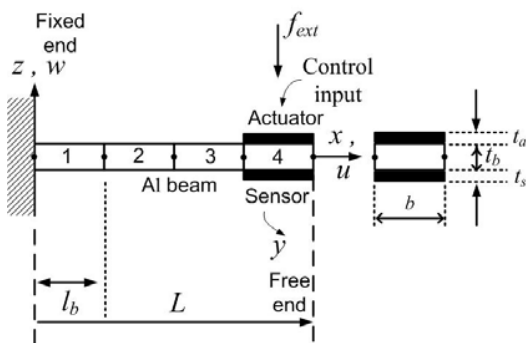


Fig. 4. A SISO smart Timoshenko beam

The displacement relation in the x, y and z directions of the beam can be written as

$$u(x, y, z, t) = z\theta(x, t) = z\left(\frac{\partial w}{\partial x} - \beta(x)\right), \quad (1)$$

$$v(x, y, z, t) = 0, \quad (2)$$

$$w(x, y, z, t) = w(x, t), \quad (3)$$

where w is the time dependent transverse displacement of the centroidal axis (along z axis), θ is the time dependent rotation of the cross-section about y axis, u is the axial displacement along the x axis, v is the lateral displacement along the y axis which is equal to zero. The total slope of the beam consists of two parts, one due to bending, which is $\theta(x)$ and the other due to shear, which is $\beta(x)$. The axial displacement of a point at a distance z from the centre line is only due to the bending slope and the shear slope has no contribution to this. The strain components of the beam are given as

$$\epsilon_{xx} = \frac{\partial u}{\partial x} = \frac{\partial}{\partial \theta} \frac{\partial \theta}{\partial x} = z \frac{\partial \theta}{\partial x}, \quad (4)$$

$$\epsilon_{yy} = \frac{\partial v}{\partial y} = 0, \quad (5)$$

$$\epsilon_{zz} = \frac{\partial w}{\partial z} = 0, \quad (6)$$

where $\epsilon_{xx}, \epsilon_{yy}, \epsilon_{zz}$ are the longitudinal strains or the tensile strains in the 3 directions, i.e., in the x, y, z directions.

The shear strains γ induced in the beam along the 3 directions (viz., along x, y, z directions) are given by

$$\gamma_{xz} = \frac{1}{2} \left[\frac{\partial u}{\partial z} + \frac{\partial w}{\partial x} \right] = \frac{1}{2} \left[\theta + \frac{\partial w}{\partial x} \right], \quad (7)$$

$$\gamma_{yz} = \frac{1}{2} \left[\frac{\partial v}{\partial z} + \frac{\partial w}{\partial y} \right] = 0, \quad (8)$$

$$\gamma_{xy} = \frac{1}{2} \left[\frac{\partial u}{\partial y} + \frac{\partial v}{\partial x} \right] = 0. \quad (9)$$

The effect of shear strains along y and z directions is equal to zero. Thus, the stresses in the beam element are given as

$$\sigma_{xx} = E \epsilon_{xx} = E z \frac{\partial \theta}{\partial x}, \quad (10)$$

$$\sigma_{xz} = G \gamma_{xz} = \frac{1}{2} G \left[\frac{\partial w}{\partial x} + \theta \right] = K \left[\frac{\partial w}{\partial x} + \theta \right], \quad (11)$$

where E is the young's modulus of the beam material, G is shear modulus (or modulus of rigidity) of the beam material, σ_{xz} is the shear stress, σ_{xx} is the tensile stress and K is the shear coefficient which depends on the material definition and on the cross sectional geometry, usually taken equal to $\frac{5}{6}$.

The strain energy of the beam element depends upon the linear strain ϵ , the shear strain γ and is given by

$$U = \frac{1}{2} EI \left(\frac{\partial \theta}{\partial x} \right)^2 + \frac{1}{2} KGA \left(\frac{\partial w}{\partial x} + \theta \right)^2 \quad (12)$$

and the total strain energy is finally written as

$$U = \frac{1}{2} \int_0^L \begin{bmatrix} \frac{\partial \theta}{\partial x} \\ \frac{\partial w}{\partial x} + \theta \end{bmatrix}^T \begin{bmatrix} EI & 0 \\ 0 & KGA \end{bmatrix} \begin{bmatrix} \frac{\partial \theta}{\partial x} \\ \frac{\partial w}{\partial x} + \theta \end{bmatrix} dx, \quad (13)$$

where I is the mass moment of inertia of the beam element, A is the area of cross section of the beam element and L is the length of the beam.

The kinetic energy T of the beam element depends on the sum of the kinetic energy due to the linear velocity \dot{w} and due to the angular twist $\dot{\theta}$ and is given by

$$T = \frac{1}{2} \rho A \left(\frac{\partial w}{\partial t} \right)^2 + \frac{1}{2} \rho I \left(\frac{\partial \theta}{\partial t} \right)^2 \quad (14)$$

and the total kinetic energy is finally written as

$$T = \frac{1}{2} \int_0^L \begin{bmatrix} \frac{\partial w}{\partial t} \\ \frac{\partial \theta}{\partial t} \end{bmatrix}^T \begin{bmatrix} \rho A & 0 \\ 0 & \rho I \end{bmatrix} \begin{bmatrix} \frac{\partial w}{\partial t} \\ \frac{\partial \theta}{\partial t} \end{bmatrix} dx, \quad (15)$$

where ρ is the mass density of the beam material.

The total work done due to the external forces in the system is given by

$$W_e = \int_0^L \begin{bmatrix} w \\ \theta \end{bmatrix}^T \begin{bmatrix} q_d \\ m \end{bmatrix} dx, \quad (16)$$

where q_d represents distributed force along the length of the beam and m represents the moment along the length of the beam.

The equation of motion is derived using the concept of the total strain energy being equal to the sum of the change in the kinetic energy and the work done due to the external forces and is given by

$$\delta \Pi = \int_{t_1}^{t_2} (\delta U - \delta T - \delta W_e) dt = 0. \quad (17)$$

Here, δU , δT and δW_e are the variations of the strain energy, the kinetic energy, work done due to the external forces and T is kinetic energy, U is strain energy, W is the external work done, L is the length of the beam element and t is the time.

Substituting the values of strain energy from (13), kinetic energy from (15) and external work done from (16) in (17) and integrating by parts, we get the governing equation of motion (Timoshenko beam equations) of a general shaped beam modeled with Timoshenko beam theory as

$$\frac{\partial \left\{ KGA \left(\frac{\partial w}{\partial x} + \theta \right) \right\}}{\partial x} + q_d = \rho A \frac{\partial^2 w}{\partial t^2}, \quad (18)$$

$$\frac{\partial \left\{ EI \frac{\partial \theta}{\partial x} \right\}}{\partial x} - KGA \left(\frac{\partial w}{\partial x} + \theta \right) + m = \rho I \frac{\partial^2 \theta}{\partial t^2}. \quad (19)$$

The R.H.S. of (18) is the time derivative of the linear momentum, whereas the R.H.S. of (19) is the time derivative of the moment of momentum.

For the static case with no external force acting on the beam, the governing equation of motion (Timoshenko beam equations) reduces to

$$\frac{\partial \left\{ KGA \left(\frac{\partial w}{\partial x} + \theta \right) \right\}}{\partial x} = 0 \quad (20)$$

and

$$\frac{\partial \left\{ EI \frac{\partial \theta}{\partial x} \right\}}{\partial x} - KGA \left(\frac{\partial w}{\partial x} + \theta \right) = 0. \quad (21)$$

From (21), it can be seen that this governing equation of the beam based on Timoshenko beam theory can only be satisfied if the polynomial order for w is selected one order higher than the polynomial order for θ .

Let w be approximated by a cubic polynomial and θ be approximated by a quadratic polynomial as

$$w = a_1 + a_2 x + a_3 x^2 + a_4 x^3, \quad (22)$$

$$\theta = b_1 + b_2 x + b_3 x^2. \quad (23)$$

Here, in (22) and (23), x is the distance of the finite element node from the fixed end of the beam, a_i and b_j ($i=1, 2, 3, 4$) and ($j=1, 2, 3$) are the unknown coefficients and are found out using the boundary conditions at the beam ends $x = (0, L)$ as

at

$$x=0, w=w_1, \theta=0 \quad (24)$$

and at

$$x=L, w=w_2, \theta=-\theta_2. \quad (25)$$

After applying boundary conditions from (24), (25) on (22), (23), the unknown coefficients a_i and b_j can be solved.

Substituting the unknown coefficients a_i and b_j in (22), (23) and writing them in matrix form, we get, the transverse displacement, the first spatial derivative of the transverse displacement, the second spatial derivative of the transverse displacement and the time derivative of (22) as

$$[w(x, t)] = [N_w] [\mathbf{q}], \quad (26)$$

$$[w'(x, t)] = [N_\theta] [\mathbf{q}], \quad (27)$$

$$[w''(x, t)] = [N_a] [\mathbf{q}], \quad (28)$$

$$[\dot{w}(x, t)] = [N_w] [\dot{\mathbf{q}}], \quad (29)$$

where \mathbf{q} is the vector of displacements and slopes, $\dot{\mathbf{q}}$ is the

time derivative of the modal coordinate vector, $[N_w]^T$, $[N_\theta]^T$, $[N_a]^T$ are the mode shape functions (for displacement, rotations and accelerations) taking the shear ϕ into consideration and are given as

$$[N_w]^T = \begin{bmatrix} \frac{1}{(1+\phi)} \left\{ 2\left(\frac{x}{L}\right)^3 - 3\left(\frac{x}{L}\right)^2 - \phi\left(\frac{x}{L}\right) + (1+\phi) \right\} \\ \frac{L}{(1+\phi)} \left\{ \left(\frac{x}{L}\right)^3 - \left(2 + \frac{\phi}{2}\right)\left(\frac{x}{L}\right)^2 + \left(1 + \frac{\phi}{2}\right)\left(\frac{x}{L}\right) \right\} \\ -\frac{1}{(1+\phi)} \left\{ 2\left(\frac{x}{L}\right)^3 - 3\left(\frac{x}{L}\right)^2 - \phi\left(\frac{x}{L}\right) \right\} \\ \frac{L}{(1+\phi)} \left\{ \left(\frac{x}{L}\right)^3 - \left(1 - \frac{\phi}{2}\right)\left(\frac{x}{L}\right)^2 - \left(\frac{\phi}{2}\right)\left(\frac{x}{L}\right) \right\} \end{bmatrix}, \quad (30)$$

$$[N_\theta]^T = \begin{bmatrix} \frac{6}{(1+\phi)L} \left\{ \left(\frac{x}{L}\right)^2 - \left(\frac{x}{L}\right) - \frac{\phi(1+\phi)}{6} + \frac{(1+\phi)^2 L}{6} \right\} \\ \frac{1}{(1+\phi)} \left\{ 3\left(\frac{x}{L}\right)^2 - (4+\phi)\left(\frac{x}{L}\right) + (1+\phi) \right\} \\ -\frac{6}{(1+\phi)L} \left\{ \left(\frac{x}{L}\right)^2 - \left(\frac{x}{L}\right) \right\} \\ \frac{1}{(1+\phi)} \left\{ 3\left(\frac{x}{L}\right)^2 - (2-\phi)\left(\frac{x}{L}\right) \right\} \end{bmatrix}, \quad (31)$$

$$[N_a]^T = \begin{bmatrix} \frac{6}{(1+\phi)L} \left\{ \frac{2x}{L^2} - \frac{1}{L} \right\} \\ \frac{1}{(1+\phi)L} \left\{ \frac{6x}{L} - (4+\phi) \right\} \\ -\frac{6}{(1+\phi)L} \left\{ \frac{6x}{L^2} - \frac{1}{L} \right\} \\ \frac{1}{(1+\phi)} \left\{ \frac{6x}{L^2} - \left(\frac{2-\phi}{L}\right) \right\} \end{bmatrix}, \quad (32)$$

where $[N_\theta] = [N_w]'$, $[N_a] = [N_w]''$, L is the length of beam element and ϕ is the ratio of the beam bending stiffness to shear stiffness and is given by

$$\phi = \frac{12}{L^2} \left(\frac{EI}{KGA} \right). \quad (33)$$

The mass matrix of the regular beam element (also called as the local mass matrix) is the sum of the translational mass and the rotational mass and is given in matrix form as

$$[M^b] = \int_0^L \begin{bmatrix} [N_w] \\ [N_\theta] \end{bmatrix}^T \begin{bmatrix} \rho A & 0 \\ 0 & \rho I_{yy} \end{bmatrix} \begin{bmatrix} [N_w] \\ [N_\theta] \end{bmatrix} dx. \quad (34)$$

Substituting the mode shape functions $[N_w]$, $[N_\theta]$ into (34) and integrating, we get the mass matrix of the regular beam element as

$$[M^b] = [M_{\rho A}] + [M_{\rho I}], \quad (35)$$

where $[M_{\rho A}]$ and $[M_{\rho I}]$ in (35) is associated with the translational inertia and rotary inertia (with the shear) as

$$[M_{\rho A}] = \frac{\rho I}{210(1+\phi)^2} \begin{bmatrix} (70\phi^2 + 147\phi + 78) & (35\phi^2 + 77\phi + 44)\frac{L}{4} \\ (35\phi^2 + 77\phi + 44)\frac{L}{4} & (7\phi^2 + 14\phi + 8)\frac{L^2}{4} \\ (35\phi^2 + 63\phi + 27) & (35\phi^2 + 63\phi + 26)\frac{L}{4} \\ -(35\phi^2 + 63\phi + 26)\frac{L}{4} & -(7\phi^2 + 14\phi + 6)\frac{L^2}{4} \\ (35\phi^2 + 63\phi + 27) & -(35\phi^2 + 63\phi + 26)\frac{L}{4} \\ (35\phi^2 + 63\phi + 26)\frac{L}{4} & -(7\phi^2 + 14\phi + 6)\frac{L^2}{4} \\ (70\phi^2 + 147\phi + 78) & -(35\phi^2 + 77\phi + 44)\frac{L}{4} \\ -(35\phi^2 + 77\phi + 44)\frac{L}{4} & (7\phi^2 + 14\phi + 8)\frac{L^2}{4} \end{bmatrix}, \quad (36)$$

$$[M_{\rho I}] = \rho I \begin{bmatrix} 36 & -(15\phi - 3)L \\ -(15\phi - 3)L & (10\phi^2 + 5\phi + 4)L^2 \\ (10\phi^2 + 5\phi + 4)L^2 & (15\phi - 3)L \\ -(15\phi - 3)L & (5\phi^2 - 5\phi - 1)L^2 \\ -36 & -(15\phi - 3)L \\ (15\phi - 3)L & (5\phi^2 - 5\phi - 1)L^2 \\ 36 & (15\phi - 3)L \\ (15\phi - 3)L & (10\phi^2 + 5\phi + 4)L^2 \end{bmatrix}. \quad (37)$$

The stiffness matrix $[K^b]$ of the regular beam element (also called as the local stiffness matrix) is the sum of the bending stiffness and the shear stiffness and is written in matrix form as

$$[K^b] = \int_0^L \begin{bmatrix} \frac{\partial}{\partial x} [N_\theta] \\ [N_\theta] + \frac{\partial}{\partial x} [N_w] \end{bmatrix}^T \begin{bmatrix} EI & 0 \\ 0 & KGA \end{bmatrix} \begin{bmatrix} \frac{\partial}{\partial x} [N_\theta] \\ [N_\theta] + \frac{\partial}{\partial x} [N_w] \end{bmatrix} dx. \quad (38)$$

Substituting the mode shape functions $[N_w]$, $[N_\theta]$ into (38) and integrating, we get the stiffness matrix of the regular beam element as $[K^b]$ which is given by

$$[K^b] = \frac{EI}{(1+\phi)L^3} \begin{bmatrix} 12 & 6L & -12 & 6L \\ 6L & (4+\phi)L^2 & -6L & (2-\phi)L^2 \\ -12 & -6L & 12 & -6L \\ 6L & (2-\phi)L^2 & -6L & (4+\phi)L^2 \end{bmatrix} \quad (39)$$

Note that when ϕ is neglected, the mass matrix and the stiffness matrix reduce to the mass and stiffness matrix of a Euler-Bernoulli beam and is shown in the appendix.

B. Finite Element Modeling of piezoelectric beam element

The regular beam elements with the piezoelectric patches are shown in Fig. 2. The piezoelectric element is obtained by bonding the regular beam element with a layer of two piezoelectric patches, one above and the other below at two finite element positions as a collocated pair. The bottom layer acts as the sensor and the top layer acts as an actuator. The element is assumed to have two structural degrees of freedom at each nodal point, which are, transverse deflection w , and an angle of rotation or slope θ and an electrical degree of

freedom, i.e., the sensor voltage.

The effect of shear is negligible in the piezoelectric patches, since they are very very thin and light as compared to the thickness of the beam. So the piezoelectric layers are modeled based on Euler-Bernoulli beam theory [28], [29] and the middle aluminum layer, i.e., the regular aluminum beam is modeled based on Timoshenko beam theory considering the effect of shear [25].

The mass matrix of the piezoelectric element is finally given by

$$[M^p] = \frac{\rho_p A_p l_p}{420} \begin{bmatrix} 156 & 22l_p & 54 & -13l_p \\ 22l_p & 4l_p^2 & 13l_p & -3l_p^2 \\ 54 & 13l_p & 156 & -22l_p \\ -13l_p & -3l_p^2 & -22l_p & 4l_p^2 \end{bmatrix}, \quad (41)$$

where

ρ_p is the mass density of piezoelectric beam element,

A_p is the area of the piezoelectric patch = $2t_a b$, i.e., the area of the sensor as well as actuator,

b being the width of the beam and

l_p is the length of the piezoelectric patch.

Similarly, we obtain the stiffness matrix $[K^{piezo}]$ of the piezoelectric element as

$$[K^p] = \frac{E_p I_p}{l_p} \begin{bmatrix} \frac{12}{l_p^2} & \frac{6}{l_p} & \frac{12}{l_p^2} & \frac{6}{l_p} \\ \frac{6}{l_p} & 4 & -\frac{6}{l_p} & 2 \\ -\frac{12}{l_p^2} & -\frac{6}{l_p} & \frac{12}{l_p^2} & -\frac{6}{l_p} \\ \frac{6}{l_p} & 2 & -\frac{6}{l_p} & 4 \end{bmatrix}, \quad (41)$$

where E_p is the modulus of elasticity of piezo material, I_p is the moment of inertia of the piezoelectric layer with respect to the neutral axis of the beam and given by

$$[I_p] = \frac{1}{12} c t_a^3 + c t_a \left(\frac{t_a + t_b}{2} \right)^2, \quad (42)$$

where t_b is the thickness of the beam and t_a is the thickness of the actuator also equal to the thickness of the sensor.

It is assumed that there is continuity of shear stress at the interface of the patches and the substrate beam.

C. Mass and stiffness of beam element with piezo patch

The mass and stiffness matrix for the piezoelectric beam element (regular beam element with piezoelectric patches placed at the top and bottom surfaces) as a collocated pair is given by

$$[M] = [M_{pA}] + [M_{pI}] + [M^p] \quad (43)$$

and

$$[K] = [K^b] + [K^p]. \quad (44)$$

Assembly of the regular beam element and the piezoelectric element is done by adding the two matrices. It is assumed that the rotations and displacements are the same in all the layers of the structure.

D. Piezoelectric strain rate sensors and actuators

The linear piezoelectric coupling between the elastic field and the electric field of a PZT material is expressed by the direct and converse piezoelectric constitutive equations as

$$D = d \sigma + e^T E_f, \quad (45)$$

$$\varepsilon = s^E \sigma + d E_f, \quad (46)$$

where σ is the stress, ε is the strain, E_f is the electric field, D is the dielectric displacement, e is the permittivity of the medium, s^E is the compliance of the medium, and d is the piezoelectric constant [31].

1) Sensor Equation

The direct piezoelectric equation is used to calculate the output charge produced by the strain in the structure. The total charge $Q(t)$ developed on the sensor surface (due to the strain) is the spatial summation of all point charges developed on the sensor layer and the corresponding current generated is given by

$$i(t) = z e_{31} c \int_0^{l_p} N_a^T \dot{q} dx, \quad (47)$$

where $z = \frac{t_b}{2} + t_a$, e_{31} is the piezoelectric stress / charge constant, \dot{q} is the time derivative of the modal coordinate vector and N_a^T is the second spatial derivative of the mode shape function of the beam.

This current is converted into the open circuit sensor voltage V^s using a signal-conditioning device with gain G_c and applied to an actuator with the controller gain K_c .

The sensor output voltage obtained is as

$$V^s = G_c e_{31} z c \int_0^{l_p} N_a^T \dot{q} dx \quad (48)$$

or can be expressed as a scalar vector product

$$V^s(t) = \mathbf{p}^T \dot{q}, \quad (49)$$

where \mathbf{p}^T is a constant vector. The input voltage to the actuator is $V^a(t)$ and is given by

$$V^a(t) = K_c G_c e_{31} z c \int_0^{l_p} N_a^T \dot{q} dx. \quad (50)$$

The cable capacitance between the piezo sensor / actuator and the signal conditioning device has been considered negligible and the temperature effects have been neglected. Note that the sensor output is a function of the second spatial derivative of the mode shape.

2) Actuator equation

The actuator strain is derived from the converse piezoelectric equation. The strain developed by the applied electric field (E_f) on the actuator layer is given by

$$\epsilon_A = d_{31} E_f = d_{31} \frac{V^a(t)}{t_a} \quad (51)$$

When the input to the actuator $V^a(t)$ is applied in the thickness direction, the stress is

$$\sigma_A = E_p d_{31} \frac{V^a(t)}{t_a} \quad (52)$$

The resultant moment M_A acting on the beam is determined by integrating the stress through the structure thickness as

$$M_A = E_p d_{31} \bar{z} V^a(t), \quad (53)$$

where \bar{z} , is the distance between the neutral axis of the beam and the piezoelectric layer. Finally, the control force applied by the actuator is obtained as

$$\mathbf{f}_{ctrl} = E_p d_{31} c \bar{z} \int_{l_p} N_\theta dx V^a(t) \quad (54)$$

or can be expressed as

$$\mathbf{f}_{ctrl} = \mathbf{h} V^a(t), \quad (55)$$

where $[N_\theta]^T$ is the first spatial derivative of mode shape function of the beam and \mathbf{h}^T is a constant vector which depends on the piezo characteristics and its location on the beam. If an external force \mathbf{f}_{ext} acts on the beam, then, the total force vector becomes

$$\mathbf{f}^t = \mathbf{f}_{ext} + \mathbf{f}_{ctrl} \quad (56)$$

E. Dynamic equation of the smart structure

The dynamic equation of the smart structure is obtained by using both the regular and piezoelectric beam elements (local matrices) given by (35), (39), (40), (41), (43) and (44). The mass and stiffness of the bonding or the adhesive between the master structure and the sensor / actuator pair is neglected. The mass and stiffness of the entire beam, which is divided into 4 finite elements with the piezo-patches placed at positions 2 and 4 is assembled using the FEM technique and the assembled matrices (global matrices), \mathbf{M} and \mathbf{K} are obtained. The equation of motion of the smart structure is finally given by

$$\mathbf{M}\ddot{\mathbf{q}} + \mathbf{K}\mathbf{q} = \mathbf{f}_{ext} + \mathbf{f}_{ctrl} = \mathbf{f}^t, \quad (57)$$

where \mathbf{M} , \mathbf{K} , \mathbf{q} , \mathbf{f}_{ext} , \mathbf{f}_{ctrl} , \mathbf{f}^t are the global mass matrix, global stiffness matrix of the smart beam, the vector of displacements and slopes, the external force applied to the beam, the controlling force from the actuator and the total force coefficient vector respectively.

The generalized coordinates are introduced into (57) using

a transformation $\mathbf{q} = \mathbf{T}\mathbf{g}$ in order to reduce it further such that the resultant equation represents the dynamics of the first two vibratory modes of the smart flexible cantilever beam. \mathbf{T} is the modal matrix containing the eigen vectors representing the first two vibratory modes. This method is used to derive the uncoupled equations governing the motion of the free vibrations of the system in terms of principal coordinates by introducing a linear transformation between the generalized coordinates \mathbf{q} and the principal coordinates \mathbf{g} . Equation (57) now becomes

$$\mathbf{M}\mathbf{T}\ddot{\mathbf{g}} + \mathbf{K}\mathbf{T}\mathbf{g} = \mathbf{f}_{ext} + \mathbf{f}_{ctrl1} + \mathbf{f}_{ctrl2}, \quad (58)$$

where \mathbf{f}_{ctrl1} and \mathbf{f}_{ctrl2} are the control force coefficient vectors to the actuators from the controller. Multiplying (58) by \mathbf{T}^T on both sides and further simplifying, we get

$$\mathbf{M}^* \ddot{\mathbf{g}} + \mathbf{K}^* \mathbf{g} = \mathbf{f}_{ext}^* + \mathbf{f}_{ctrl1}^* + \mathbf{f}_{ctrl2}^*, \quad (59)$$

where $\mathbf{M}^* = \mathbf{T}^T \mathbf{M} \mathbf{T}$, $\mathbf{K}^* = \mathbf{T}^T \mathbf{K} \mathbf{T}$, $\mathbf{f}_{ext}^* = \mathbf{T}^T \mathbf{f}_{ext}$ and $\mathbf{f}_{ctrli}^* = \mathbf{T}^T \mathbf{f}_{ctrli}$, $i = 1$ to 2 .

Here, the parameters \mathbf{M}^* , \mathbf{K}^* , \mathbf{f}_{ext}^* , \mathbf{f}_{ctrl1}^* , \mathbf{f}_{ctrl2}^* represents the generalized mass matrix, the generalized stiffness matrix, the generalized external force vector and the generalized control force vectors respectively. The generalized structural modal damping matrix \mathbf{C}^* is introduced into (59) by using

$$\mathbf{C}^* = \alpha \mathbf{M}^* + \beta \mathbf{K}^*, \quad (60)$$

where α and β are the frictional damping constant and the structural damping constant used in \mathbf{C}^* . The dynamic equation of the smart flexible cantilever beam developed is obtained as

$$\mathbf{M}^* \ddot{\mathbf{g}} + \mathbf{C}^* \dot{\mathbf{g}} + \mathbf{K}^* \mathbf{g} = \mathbf{f}_{ext}^* + \mathbf{f}_{ctrl}^*, \quad (61)$$

where $\mathbf{f}_{ctrl}^* = \mathbf{f}_{ctrl1}^* + \mathbf{f}_{ctrl2}^*$.

F. State Space Model of the Smart Structure

The state space model of the smart flexible cantilever beam is obtained as follows [25], [36].

Let
$$\mathbf{g} = \begin{bmatrix} x_1 \\ x_2 \end{bmatrix} \Rightarrow \dot{\mathbf{g}} = \begin{bmatrix} \dot{x}_1 \\ \dot{x}_2 \end{bmatrix} = \begin{bmatrix} x_3 \\ x_4 \end{bmatrix}, \quad (62)$$

Thus,
$$\dot{x}_1 = x_3, \quad \dot{x}_2 = x_4 \quad (63)$$

and (61) now becomes

$$\mathbf{M}^* \begin{bmatrix} \dot{x}_3 \\ \dot{x}_4 \end{bmatrix} + \mathbf{C}^* \begin{bmatrix} x_3 \\ x_4 \end{bmatrix} + \mathbf{K}^* \begin{bmatrix} x_1 \\ x_2 \end{bmatrix} = \mathbf{f}_{ext}^* + \mathbf{f}_{ctrl}^*, \quad (64)$$

which can be further simplified as

$$\begin{bmatrix} \dot{x}_3 \\ \dot{x}_4 \end{bmatrix} = -\mathbf{M}^{*-1} \mathbf{K}^* \begin{bmatrix} x_1 \\ x_2 \end{bmatrix} - \mathbf{M}^{*-1} \mathbf{C}^* \begin{bmatrix} x_3 \\ x_4 \end{bmatrix} + \mathbf{M}^{*-1} \mathbf{f}_{ext}^* + \mathbf{M}^{*-1} \mathbf{f}_{ctrl}^*. \quad (65)$$

The generalized external force coefficient vector is

$$\begin{aligned} \mathbf{f}_{ext}^* &= \mathbf{T}^T \mathbf{f}_{ext}, \\ &= \mathbf{T}^T f r(t), \end{aligned} \quad (66)$$

where $r(t)$ is external force input (impulse disturbance) to the beam.

The generalized control force coefficient vector is

$$\begin{aligned} \mathbf{f}_{ctrl i}^* &= \mathbf{T}^T f_{ctrl i}, \quad i=1 \text{ to } 2, \\ &= \mathbf{T}^T \mathbf{h}_i V_i^a(t), \\ &= \mathbf{T}^T \mathbf{h}_i u_i(t), \end{aligned} \quad (67)$$

where the voltages $V_i^a(t)$ are the input voltages to the actuators 1 and 2 from the controllers respectively, and are nothing but the control inputs $u_i(t)$ to the actuators, \mathbf{h}_i is a constant vector which depends on the actuator type, its characteristics and its position on the beam and is given by

$$\begin{aligned} \mathbf{h}_1 &= E_p d_{31} b \bar{z} [-1 \quad 1 \quad \dots \quad 0 \quad 0]_{8 \times 1}, \\ &= a_c [-1 \quad 1 \quad \dots \quad 0 \quad 0] \end{aligned} \quad (68)$$

for one piezoelectric actuator element (say, for the piezo patch placed at the finite element position numbering 2), where $E_p d_{31} b \bar{z} = a_c$ being the actuator constant. So, using (63), (66) and (67) in (65), the state space equation for the smart beam is represented as

$$\begin{aligned} \begin{bmatrix} \dot{x}_1 \\ \dot{x}_2 \\ \dot{x}_3 \\ \dot{x}_4 \end{bmatrix} &= \begin{bmatrix} 0 & I \\ -\mathbf{M}^{*-1} \mathbf{K}^* & -\mathbf{M}^{*-1} \mathbf{C}^* \end{bmatrix}_{(4 \times 4)} \begin{bmatrix} x_1 \\ x_2 \\ x_3 \\ x_4 \end{bmatrix} + \\ &\begin{bmatrix} 0 & 0 \\ \mathbf{M}^{*-1} \mathbf{T}^T \mathbf{h}_1 & \mathbf{M}^{*-1} \mathbf{T}^T \mathbf{h}_2 \end{bmatrix}_{(4 \times 2)} \begin{bmatrix} u_1 \\ u_2 \end{bmatrix} \\ &+ \begin{bmatrix} 0 \\ \mathbf{M}^{*-1} \mathbf{T}^T \mathbf{f} \end{bmatrix}_{(4 \times 1)} r(t), \end{aligned} \quad (69)$$

$$\text{i.e.,} \quad \dot{\mathbf{X}} = \mathbf{A} \mathbf{x}(t) + \mathbf{B} \mathbf{u}(t) + \mathbf{E} r(t). \quad (70)$$

The sensor voltage is taken as the output of the system and its equation (output equation) is modeled as

$$V_i^s(t) = \mathbf{p}_i^T \dot{\mathbf{q}} = y_i(t), \quad i=1 \text{ to } 2, \quad (71)$$

where \mathbf{p}_i^T is a constant vector which depends on the type of the piezoelectric sensor, its characteristics (i.e., the sensor constant S_c) and on the position of the sensor location on the beam. The constant vector for the sensor placed at finite element position numbering 4 is and is given by

$$\begin{aligned} \mathbf{p}_2^T &= G_c e_{31} z b [0 \quad 0 \quad \dots \quad -1 \quad 1]_{1 \times 8}, \\ &= S_c [0 \quad 0 \quad \dots \quad -1 \quad 1], \end{aligned} \quad (72)$$

where $G_c e_{31} z b = S_c$ is the sensor constant.

Thus, the sensor output for a MIMO case is given by

$$y(t) = \mathbf{p}^T \dot{\mathbf{q}} = \mathbf{p}^T \mathbf{T} \dot{\mathbf{g}} = \mathbf{p}^T \mathbf{T} \begin{bmatrix} x_3 \\ x_4 \end{bmatrix}, \quad (73)$$

which can be written as

$$\begin{bmatrix} y_1 \\ y_2 \end{bmatrix} = \begin{bmatrix} 0 & \mathbf{p}_1^T \\ 0 & \mathbf{p}_2^T \end{bmatrix}_{(2 \times 4)} \begin{bmatrix} x_1 \\ x_2 \\ x_3 \\ x_4 \end{bmatrix} \quad (74)$$

for a multivariable case with 2 inputs and 2 outputs.

$$\text{i.e.,} \quad y(t) = \mathbf{C}^T \mathbf{x}(t) + \mathbf{D} \mathbf{u}(t). \quad (75)$$

which is the output equation.

The multivariable state space model (state equation and the output equation) of the smart structure developed for the system in (70) and (75) thus, is given by

$$\begin{aligned} \dot{\mathbf{x}} &= \mathbf{A} \mathbf{x}(t) + \mathbf{B} \mathbf{u}(t) + \mathbf{E} r(t), \\ y(t) &= \mathbf{C}^T \mathbf{x}(t) + \mathbf{D} \mathbf{u}(t), \end{aligned} \quad (76)$$

with

$$\begin{aligned} \mathbf{A} &= \begin{bmatrix} 0 & I \\ -\mathbf{M}^{*-1} \mathbf{K}^* & -\mathbf{M}^{*-1} \mathbf{C}^* \end{bmatrix}_{(4 \times 4)}, \quad \mathbf{D} = \text{Null Matrix}, \\ \mathbf{B} &= \begin{bmatrix} 0 & 0 \\ \mathbf{M}^{*-1} \mathbf{T}^T \mathbf{h}_1 & \mathbf{M}^{*-1} \mathbf{T}^T \mathbf{h}_2 \end{bmatrix}_{(4 \times 2)}, \\ \mathbf{C}^T &= \begin{bmatrix} 0 & \mathbf{p}_1^T \\ 0 & \mathbf{p}_2^T \end{bmatrix}_{(2 \times 4)}, \quad \mathbf{E} = \begin{bmatrix} 0 \\ \mathbf{M}^{*-1} \mathbf{T}^T \mathbf{f} \end{bmatrix}_{(4 \times 1)}, \end{aligned} \quad (77)$$

where $r(t), u(t), \mathbf{A}, \mathbf{B}, \mathbf{C}, \mathbf{D}, \mathbf{E}, \mathbf{x}(t)$ and $y(t)$ represents the external force input, the control input, system matrix, input matrix, output matrix, transmission matrix, external load matrix, state vector, system output (sensor output).

By making 2 piezoelectric elements as active sensors / actuators at a time and by making other elements as regular beam elements, control of this MIMO state space model is obtained using the periodic output feedback control technique which is considered in the next section. The characteristics of smart flexible MIMO cantilever beam are given in Table 3.

TABLE III
 CHARACTERISTICS OF THE SMART FLEXIBLE MIMO BEAM

Position of sensor / actuator	Eigen values	Natural Freq. (Hz)
	$-0.61 \pm j 123.68$	19.68
Elements 2, 4	$-2.35 \pm j 762.43$	121.34

IV. DESIGN OF THE POF CONTROLLER

In the following section, we develop the control strategy for the multivariable representation of the developed smart

structure model using the periodic output feedback control law [13]-[15], [24], [37], [38] with 2 actuator inputs u_1, u_2 and 2 sensor outputs y_1, y_2 for the MIMO smart structure plant as shown in Fig. 3. The problem of pole assignment by piecewise constant output feedback was studied by Chammas and Leondes [13]-[15] for LTI systems with infrequent observations. They have shown that by the use of a periodically time-varying piecewise constant output feedback gain, the poles of the discrete time control system could be assigned arbitrarily (within the natural restriction that they should be located symmetrically with respect to the real axis) using the POF technique. Since the feedback gains are piecewise constants, their method could easily be implemented, guarantees the closed loop stability and indicated a new possibility. Such a control law can stabilize a much larger class of systems.

A. A brief review of the periodic output feedback control technique

Consider a LTI CT system [13]-[15], [24], [37], [38] given by

$$\begin{aligned} \dot{x} &= Ax + Bu, \\ y &= Cx, \end{aligned} \quad (78)$$

which is sampled with a sampling interval of τ secs given by the discrete linear time invariant system (called as the tau system) as

$$\begin{aligned} x(k+1) &= \Phi_\tau x(k) + \Gamma_\tau u(k), \\ y(k) &= Cx(k), \end{aligned} \quad (79)$$

where $x \in \mathfrak{R}^n, u \in \mathfrak{R}^m, y \in \mathfrak{R}^p$ and Φ_τ, Γ_τ and C are constant matrices of appropriate dimensions. The following control law is applied to this system. The output y is measured at the time instant $t = k\tau, k = 0, 1, 2, \dots$. We consider constant hold function because they are more suitable for implementation. An output-sampling interval is divided into N sub-intervals of length $\Delta = \tau/N$ and the hold function is assumed to be constant on these sub-intervals as shown in the Fig. 5. Thus, the control law becomes

$$\begin{aligned} u(t) &= K_l y(k\tau), \\ (k\tau + l\Delta) \leq t \leq (l+1)\Delta, \quad K_{l+N} &= K_l \end{aligned} \quad (80)$$

for $l = 0, 1, 2, \dots, (N-1)$. Note that a sequence of N gain matrices $\{K_0, K_1, \dots, K_{N-1}\}$, when substituted in (80), generates a time-varying piecewise constant output feedback gain $\mathbf{K}(t)$ for $0 \leq t \leq \tau$.

Consider the following system, which is obtained by sampling the system in (78) at sampling interval of $\Delta = \tau/N$ and denoted by (Φ, Γ, C) called as the delta system :

$$\begin{aligned} x(k+1) &= \Phi x(k) + \Gamma u(k), \\ y(k) &= Cx(k), \end{aligned} \quad (81)$$

Assume (Φ_τ, C) is observable and (Φ, Γ) is controllable with controllability index ν such that $N \geq \nu$, then it is possible to choose a gain sequence K_l , such that the closed-loop system, sampled over τ , takes the desired self-conjugate set of eigen values.

Define

$$\mathbf{K} = \begin{bmatrix} K_0 \\ K_1 \\ K_2 \\ \vdots \\ K_{N-1} \end{bmatrix}, \quad (82)$$

$$\mathbf{u}(k\tau) = \mathbf{K} y(k\tau) = \begin{bmatrix} u(k\tau) \\ u(k\tau + \Delta) \\ \vdots \\ u(k\tau + \tau - \Delta) \end{bmatrix}, \quad (83)$$

then, a state space representation for the system sampled over τ is

$$\begin{aligned} x(k\tau + \tau) &= \Phi^N x(k\tau) + \Gamma u(k\tau), \\ y(k\tau) &= Cx(k\tau), \end{aligned} \quad (84)$$

where $\Gamma = [\Phi^{N-1}\Gamma, \dots, \Gamma]$.

Applying POF in (80), i.e., $\mathbf{K} y(k\tau)$ is substituted for $\mathbf{u}(k\tau)$, the closed loop system becomes

$$x(k\tau + \tau) = (\Phi^N + \Gamma \mathbf{K} C) x(k\tau). \quad (85)$$

The problem has now taken the form of static output feedback [33], [39]. Equation (85) suggests that an output injection matrix G be found such that

$$\rho(\Phi^N + GC) < 1, \quad (86)$$

where $\rho(\cdot)$ denotes the spectral radius. By observability, one can choose an output injection gain G to achieve any desired self-conjugate set of eigen values for the closed-loop matrix $(\Phi^N + GC)$ and from $N \geq \nu$, it follows that one can find a POF gain which realizes the output injection gain G by solving

$$\Gamma \mathbf{K} = G \quad (87)$$

for \mathbf{K} . The controller obtained from this equation will give the desired behaviour, but might require excessive control action. To reduce this effect, we relax the condition that \mathbf{K} exactly satisfy the linear equation and include a constraint on it.

Thus, we arrive at the following in the inequality equations :

$$\|\mathbf{K}\| < \rho_1, \quad (88)$$

$$\|\Gamma \mathbf{K} - G\| < \rho_2. \quad (89)$$

Using the schur complement, it is straight forward to bring these conditions in the form of linear matrix inequalities [39], [19] as

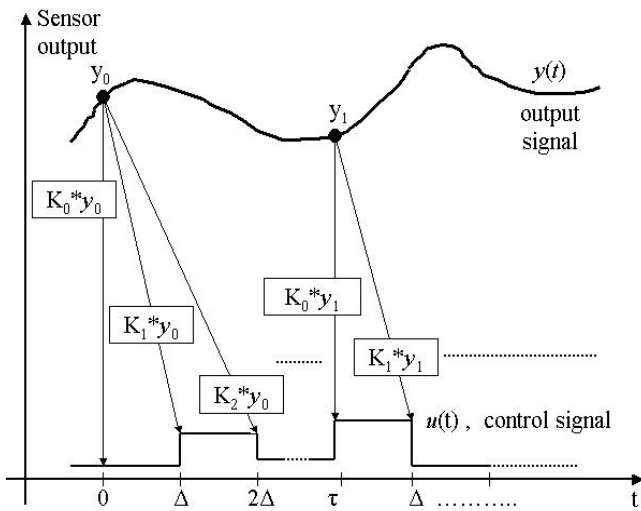


Fig. 5 Graphical illustration of the POF control law

$$\begin{bmatrix} -\rho_1^2 I & \mathbf{K} \\ \mathbf{K}^T & -I \end{bmatrix} < 0, \quad (90)$$

$$\begin{bmatrix} -\rho_2^2 I & (\mathbf{\Gamma} \mathbf{K} - \mathbf{G}) \\ (\mathbf{\Gamma} \mathbf{K} - \mathbf{G})^T & -I \end{bmatrix} < 0. \quad (91)$$

In this form, the LMI toolbox of MATLAB can be used for the synthesis of \mathbf{K} [19], [39]. The POF controller obtained by this method requires only constant gains and is hence easier to implement. In the latter case, Werner and Furuta [37], [38] proposed a performance index so that $\mathbf{\Gamma} \mathbf{K} = \mathbf{G}$ need not be forced exactly.

This constraint is replaced by a penalty function, which makes it possible to enhance the closed loop performance by allowing slight deviations from the original design and at the same time improving the behaviour. The performance index $J(k)$ is given by

$$J(k) = \sum_{i=0}^{\infty} \begin{bmatrix} x_i^T & u_i^T \end{bmatrix} \begin{bmatrix} \bar{Q} & 0 \\ 0 & R \end{bmatrix} \begin{bmatrix} x_i \\ u_i \end{bmatrix} + \sum_{k=1}^{\infty} (x_{kN} - x_{kN}^*)^T \bar{P} (x_{kN} - x_{kN}^*), \quad (92)$$

where $R \in \mathfrak{R}^{m \times m}$, $\bar{Q}, \bar{P} \in \mathfrak{R}^{n \times n}$ are positive definite and symmetric weight matrices, x_i and u_i denote the states and the inputs of the delta system respectively and x_{kN}^* denotes the state that would be reached at the instant kN , given $x_{(k-1)N}$, if K is solved to satisfy (87) exactly, i.e., $x_{kN}^* = (\mathbf{\Phi}^N + \mathbf{G} \mathbf{C}) x_{(k-1)N}$.

The first term represents the 'averaged' state and control energy whereas the second term penalizes the deviation of G . A trade-off between the closed loop performance and closeness to the chosen design is expressed by the above cost

function.

V. CONTROL SIMULATIONS OF THE BEAM

The FEM and the state space model of the smart cantilever beam is developed in MATLAB using Timoshenko beam theory. The cantilever beam is divided into 4 finite elements and the sensor and actuator as collocated pairs are placed at finite element positions 2 and 4 respectively, thus giving rise to a single MIMO model of the smart structure plant.

A fourth order state space model of the system is obtained on retaining the first two dominant modes of vibration of the system. The POF control technique discussed in the previous section is used to design a controller to suppress the first two vibration modes of a cantilever beam through smart structure concept. Simulations are carried out in MATLAB. The performance of the system is evaluated for vibration control.

An external force \mathbf{f}_{ext} (impulse disturbance) of 1 Newton is applied for duration of 50 ms at the free end of the beam shown in Fig. 3 and the open loop response of the system is observed. The first task in designing the POF controller is the selection of the sampling interval τ .

The maximum bandwidth for all the sensor / actuator locations on the beam are calculated (here, the second vibratory mode of the plant) and then by using existing empirical rules for selecting the sampling interval based on bandwidth, approximately 10 times of the maximum second vibration mode frequency of the system has been selected.

The sampling interval used is $\tau = 0.004$ seconds. Let $(\mathbf{\Phi}_\tau, \mathbf{\Gamma}_\tau, \mathbf{C})$ be the discrete time system (tau system) of the system in Fig. 3 given in (76) sampled at a rate of $1/\tau$ seconds respectively.

It is found that the DT systems are controllable and observable. The ranks of the matrices are 4. The stabilizing output injection gains are obtained for the tau system such that the eigenvalues of $(\mathbf{\Phi}_i^N + \mathbf{G}_i \mathbf{C}_i)$ lie inside the unit circle and the response of the system has a good settling time. The impulse response of the system with the output injection gain G is observed.

Let $(\mathbf{\Phi}, \mathbf{\Gamma}, \mathbf{C})$ be the discrete time system (delta system) of the system in Fig. 3 in (76) sampled at the rate of $1/\Delta$ secs respectively, where $\Delta = \tau / N$. The number of sub-intervals, N is chosen to be 10.

The periodic output feedback gain matrix \mathbf{K} for the smart system given is obtained by solving $\mathbf{\Gamma} \mathbf{K} = \mathbf{G}$ using the LMI optimization method [19], [39] which reduces the amplitude of the control signal u . With the designed controller put in the loop, the closed loop impulse responses (sensor outputs y_1 and y_2) with the periodic output feedback gain \mathbf{K} of the system are observed.

The variation of the control signal u_1 and u_2 with time for the MIMO model shown in the Fig. 3 are also observed. The tip displacements are also observed with and without the

controller.

Simulations are also performed for the SISO based smart structure shown in the Fig. 4 and the open loop response, closed loop responses with G and K , the control input and the tip displacements are also observed. The MIMO and the SISO results are compared and the conclusions are drawn.

The POF gain matrix K for the MIMO model of the smart beam is given by

$$\mathbf{K}^T = 10^2 * \begin{bmatrix} -0.45 & 0.23 & -0.35 & -0.49 & 0.56 \\ -0.46 & 0.28 & -0.39 & -0.51 & 0.59 \\ -0.72 & 0.89 & 0.93 & 0.87 & 0.41 \\ -0.76 & 0.98 & 1.01 & 1.04 & 0.97 \end{bmatrix} = [\mathbf{K}_1^T \quad \mathbf{K}_2^T] \quad (93)$$

VI. SIMULATION RESULTS

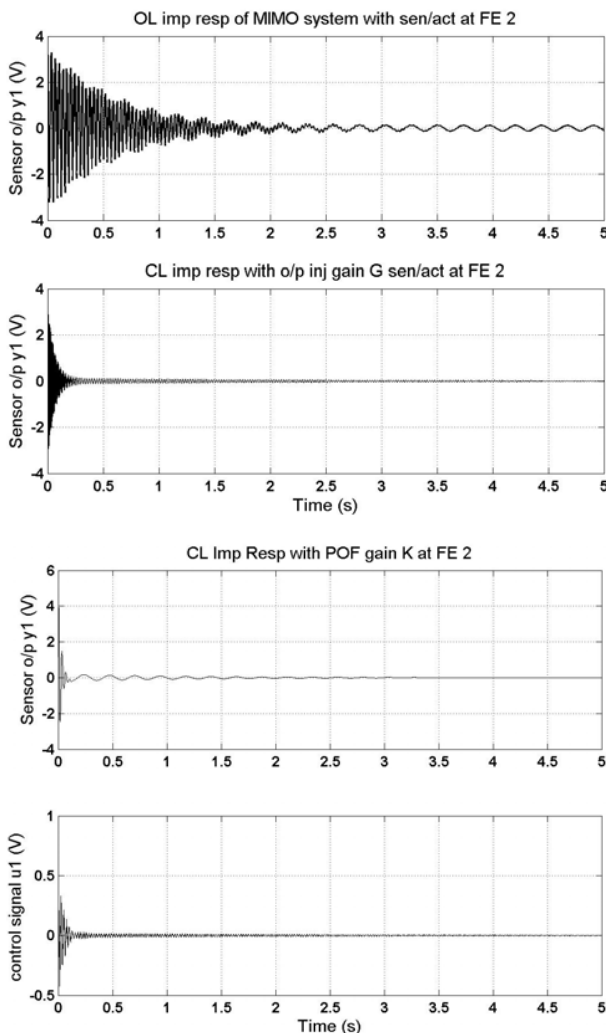


Fig. 6 Open loop, Closed loop responses (with output injection gain G_1 , POF gain K_1), control input u_1 of the MIMO beam (piezo patch placed at finite element position 2)

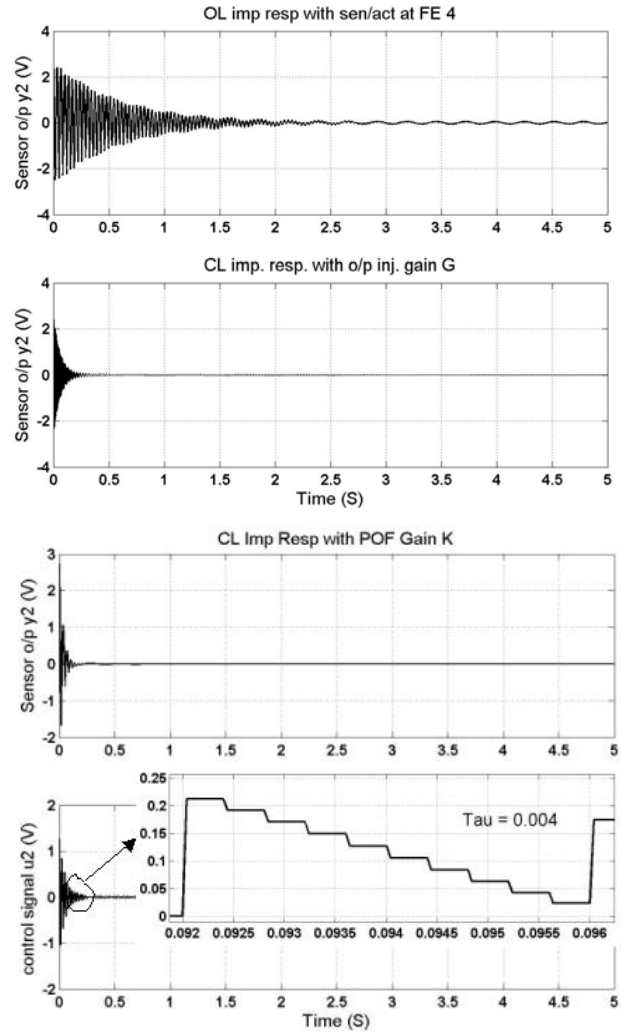


Fig. 7 Open loop, Closed loop responses (with output injection gain G_2 , POF gain K_2), control input u_2 of the MIMO beam (piezo patch placed at finite element position 4)

The open loop response, the closed loop response with the output injection gain G_1 , the closed loop response y_1 with the POF gain K_1 , the control input u_1 of the MIMO system for the sensor / actuator pair placed at finite element position 2 are shown in Fig. 6. Similarly, the open loop response, the closed loop response with the output injection gain G_2 , the closed loop response y_2 with the POF gain K_2 , the control input u_2 of the MIMO system for the sensor / actuator pair placed at finite element position 4 are shown in Fig. 7.

The open loop response, the closed loop response with the output injection gain G , the closed loop response with the POF gain K , the control input u of the SISO system is shown in Fig. 8. The tip displacements for the MIMO system and the SISO without and with the POF controller are shown in Figs. 9 and 10 respectively.

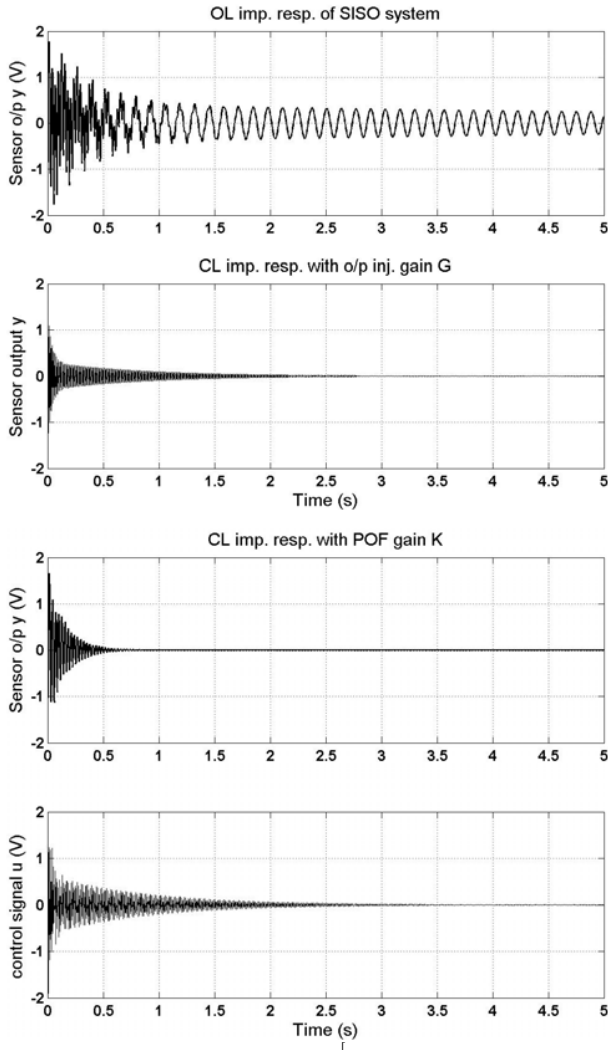


Fig. 8 OL, CL responses (with output injection gain G and POF gain K), control input u for SISO beam with piezo patch placed at FE position 4

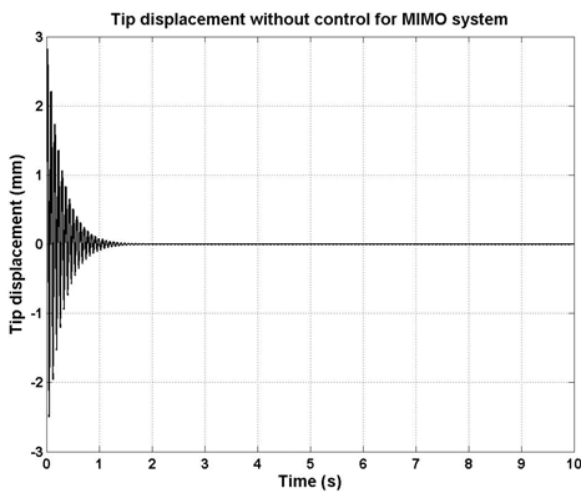


Fig. 9 (a) Tip displacements of the MIMO beam without the POF controller

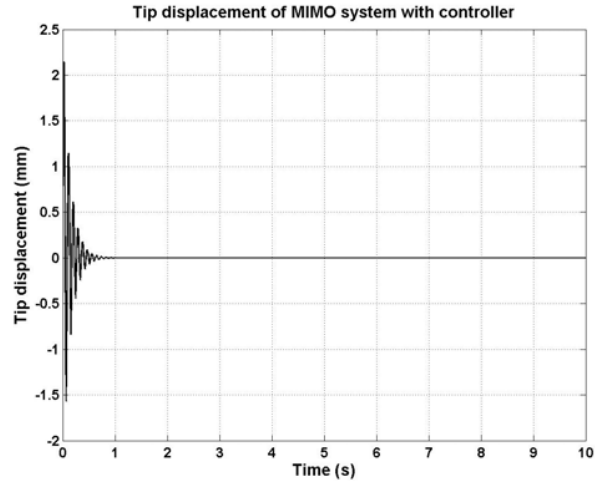


Fig. 9 (b) Tip displacement of the MIMO beam with the POF controller

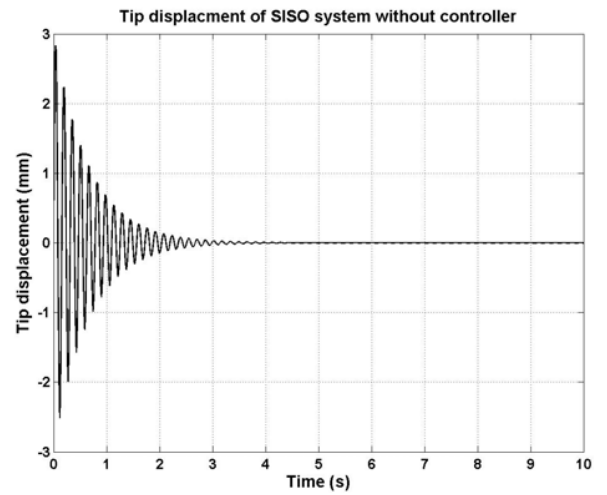


Fig. 10 (a) Tip displacements of the SISO beam without the POF controller

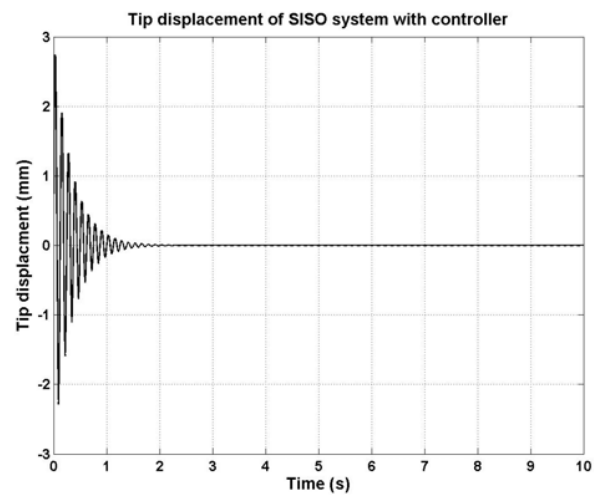


Fig. 10 (b) Tip displacements of the SISO beam without and with the POF controller

VII. CONCLUSIONS

Periodic output feedback controller has been designed for the MIMO smart structure state space model. The beam was divided into 4 finite elements with sensor / actuator pair placed at finite element positions 2 and 4. The various responses are obtained for the designed state space model. Through the simulation results, it is shown that when the plant is placed with this controller, the plant performs well. It is also observed that modeling a smart structure by including the sensor / actuator mass and stiffness and by placing the sensor / actuator at two different positions introduces a considerable change in the structural vibration characteristics.

In this paper, for the multivariable case, it is observed that when the pair is kept at two different locations, the open loop and closed loop responses of the MIMO system is less oscillatory compared to the single input single output case. The response takes lesser time to settle than the SISO case. The control effort u required is also less. The impulse responses with the output injection gain G and the POF gain \mathbf{K} shows better performance. As the bending moment is distributed heavily near the fixed end for the fundamental mode, this leads to a large strain (strain rate being very high) and results in high sensor output voltage.

The sensor voltage is greater when the pair is located near by the fixed end (FE position 2). The control effort required gets reduced if sensor / actuator locations are moved towards the fixed end. The sensor voltage is very less when the pair is located at the free end (FE position 4). Hence, a large control effort is required to damp out the vibrations in this case. Also it is inferred that, the sensor / actuator pair sensitivity depends on its placement position and the mode number. The output injection gain for the multivariable plant is obtained so that its poles are inside the unit circle and has a good settling time of less than 1 second.

The pair kept at position 2 controls the two vibratory modes at that finite element position 2, while the pair kept at position 4 also controls the two vibratory modes, but placed at that finite element position 4. A overall better performance of the system is obtained than in the SISO case [25]. In this case, the output takes lesser time to settle, vibrations are damped out quickly. The control effort required is less. In the SISO case [30], the response takes little more time to settle. Hence, it can be concluded that multivariable control of a smart structure is better compared to the single input single output control as

- the two vibratory modes can be suppressed to a larger extent at two different finite element positions and
- the response characteristics with G and with \mathbf{K} also are improved
- the tip displacements are improved and the vibrations dampen out quickly in this case.
- multiple interactions of the input and the output.

MIMO dynamic analysis is able to identify pairs of modes that occur at nearly identical frequencies. SISO experiments are not actually reliable when it comes to accurate

identification of mode pairs because they are unable to positively decipher mode pairs from signal noise in the measured Frequency Response Functions (FRF). For example, mode pair at 19.26 Hz and 19.94 Hz of the first natural frequency in MIMO was originally interpreted as a single mode at 19.68 Hz in SISO.

Depending on the application, the smearing of the mode pairs into single modes may adversely affect the control algorithm, depending on the algorithm's sensitivity to the identified resonant frequencies of the system. MIMO excitation is better than SISO excitation as only exciting at a single point may cause poor distribution of input energy throughout the structure and may result in somewhat slightly disturbed frequency responses. A multi input test provides better energy distribution and even better actuation forces.

Responses are obtained without control and are compared with the control to show the control effect. From the simulations, it was observed that without control the transient response was predominant and with control, the vibrations are suppressed. Thus, an integrated finite element model to analyze the vibration suppression capability of a smart cantilever beam with surface mounted piezoelectric devices based on Timoshenko beam theory is presented in this paper.

The limitations of Euler-Bernoulli beam theory such as the neglect of the shear ϕ and axial displacements have been considered here while modeling the beam. Timoshenko beam theory corrects the simplifying assumptions made in Euler-Bernoulli beam theory and the model obtained can be a exact one. The designed POF controller requires constant gains and hence is easier to implement in real time.

APPENDIX

When ϕ is neglected, the mass matrix reduces to

$$[M_{\rho A}] = \frac{\rho I}{210} \begin{bmatrix} 78 & 11L & 27 & -13 \frac{L}{2} \\ 11L & 2L^2 & 13 \frac{L}{2} & -3 \frac{L^2}{2} \\ 27 & 13 \frac{L}{2} & 78 & -11L \\ -13 \frac{L}{2} & -3 \frac{L^2}{2} & -11L & 2L^2 \end{bmatrix},$$

which can be written as

$$= \frac{\rho I}{420} \begin{bmatrix} 156 & 22I_b & 54 & -13L \\ 22L & 4L^2 & 13L & -3L^2 \\ 54 & 13L & 156 & -22L \\ -13L & -3L^2 & -22L & 4L^2 \end{bmatrix}.$$

When ϕ is neglected, the stiffness matrix reduces to

$$[K] = \frac{EI}{L^3} \begin{bmatrix} 12 & 6L & -12 & 6L \\ 6L & 4L^2 & -6L & 2L^2 \\ -12 & -6L & 12 & -6L \\ 6L & 2L^2 & -6L & 4L^2 \end{bmatrix}.$$

The mode shape function ϕ when neglected reduces to

$$[N_w]^T = \begin{bmatrix} 1 - 3\frac{x^2}{l_b^2} + 2\frac{x^3}{l_b^3} \\ x - 2\frac{x^2}{l_b} + \frac{x^3}{l_b^2} \\ 3\frac{x^2}{l_b^2} - 2\frac{x^3}{l_b^3} \\ -\frac{x^2}{l_b} + \frac{x^3}{l_b^2} \end{bmatrix}$$

ACRONYMS / ABBREVIATIONS

SISO	Single Input Single Output
MIMO	Multi Input Multi Output
FEM	Finite Element Method
FE	Finite Element
LMI	Linear Matrix Inequalities
MR	Magneto Rheological
ER	Electro Rheological
PVDF	Poly Vinylidene Fluoride
CF	Clamped Free
CC	Clamped Clamped
CT	Continuous Time
DT	Discrete Time
HOBT	Higher Order Beam Theory
RHS	Right Hand Side
LTI	Linear Time Invariant
POF	Periodic Output Feedback
EB	Euler-Bernoulli
PZT	Lead Zirconate Titanate
IEEE	Institute of Electrical & Electronics Engineers
IOP	Institute of Physics
ISSS	Institute of Smart Structures and Systems
SPIE	Society of Photonics & Instrumentation Engineers

NOMENCLATURE (LIST OF SYMBOLS)

f_{ext}	External force input
l	Length of the beam
b	Width of the beam
E_b	Young's modulus of beam
ρ, ρ_b	Mass density of beam
α, β	Structural constants
t_b	Thickness of beam
l_p	Length of the piezoelectric patch
t_a	Thickness of actuator
t_s	Thickness of sensor
E_p	Young's modulus of piezoelectric
ρ_p	Mass density of piezoelectric
d_{31}	Piezoelectric strain constant

g_{31}	Piezoelectric stress constant
θ	Bending angle (rotation about Y axis)
β	Shear angle
X, Y and Z	The 3 axis of 3D space
u	Axial displacement along X axis
v	Lateral displacement along the Y axis
T, U	Kinetic energy and strain energy
σ_{xz}, σ_{xx}	Shear stress, Tensile stress
K	Shear coefficient
ε	Linear strain
γ	Shear strain
I	Mass MI of beam element
A	Area of cross section of beam element
\dot{w}	Linear velocity
q_d	Distributed force along length of the beam
m	Moment along the length of the beam
W_e	Work done due to the external forces
W	External work done
t	Time in secs
a_i	Unknown coefficients ($i=1, 2, 3, 4$)
b_j	Unknown coefficients ($j=1, 2, 3$)
\mathbf{q}	Vector of displacements and slopes
$\dot{\mathbf{q}}$	Time derivative of the modal coordinate
vector E_f	Electric field
D	Dielectric displacement
e	Permittivity of the medium
s^E	Compliance of the medium
d	Piezoelectric constant
$Q(t)$	Charge developed on the sensor surface
$i(t)$	Current generated by the sensor surface
	Piezoelectric stress / charge constant
V^s	Sensor voltage V^s
G_c	Signal-conditioning device with gain
K_c	Controller gain K_c
$y(t)$	Output of the system (sensor output)
$V^a(t)$	Actuator voltage
$V^s(t)$	Sensor voltage
\mathbf{f}_{ctrl}	Control force applied by the actuator
\mathbf{f}^t	Total force coefficient vector
\mathbf{M}^*	Generalized mass matrix
\mathbf{K}^*	Generalized stiffness matrix
\mathbf{C}^*	Generalized damping matrix
\mathbf{g}	Principal coordinates

$u(t)$	Control input
$r(t)$	External input to the system
$x(t)$	State vector
$\dot{x}(t)$	Derivative of the state vector
\mathfrak{R}^n	n dimension space
τ	Sampling interval
G	Output injection gain
ν	Controllability index of the system
u_k, y_k	Input and output at the k^{th} instant
C_0, D_0	Lifted system matrices
ρ_1, ρ_2, ρ_3	Spectral norms
I	Identity matrix
N	Number of sub-intervals
L	Length of beam element
M^p	Mass matrix of the piezoelectric element
A_p	Area of the piezoelectric patch
$[M_{\rho I}]$	Mass matrix with rotary inertia
ϕ	Ratio of beam bending stiffness to shear stiffness
$[N_w]^T$	Mode shape functions for displacement taking ϕ into consideration
K^p	Stiffness matrix of piezoelectric element
$[N_\theta]^T$	Mode shape functions for rotations taking ϕ into consideration
$[N_a]^T$	Mode shape functions for accelerations taking ϕ into consideration
K^b	Stiffness matrix of the regular beam element (also called as the local stiffness matrix)
M^b	Mass matrix of the regular beam element (also called as the local Mass matrix)
$[M_{\rho A}]$	Mass matrix associated with translational inertia
$\epsilon_{xx}, \epsilon_{yy}, \epsilon_{zz}$	Longitudinal strains or the tensile strains in the 3 directions
Φ_τ, Γ_τ	System matrix, input matrix discretized at sampling interval of τ secs
Φ, Γ	System matrix, input matrix discretized at sampling interval of Δ secs
A, B, C, D	State space system matrices (CT)
E	External load matrix which couples the disturbance to the system
M, K	Mass and stiffness of the regular beam element
p^T	Constant vector, which depends on sensor

characteristics

h^T	Constant vector, which depends on actuator characteristics
M	Assembled mass matrices (global mass matrix)
K	Assembled stiffness matrices (global stiffness matrix), Periodic output feedback gain
T	Modal matrix containing the eigenvectors representing the 1 st 2 modes

REFERENCES

- [1] O. J. Aldraihem, R. C. Wetherhold, and T. Singh, "Distributed control of laminated beams : Timoshenko Vs. Euler-Bernoulli Theory," *J. of Intelligent Materials Systems and Structures*, vol. 8, pp. 149–157, 1997.
- [2] H. Abramovich, "Deflection control of laminated composite beam with piezoceramic layers-Closed form solutions," *Composite Structures*, vol. 43, no. 3, pp. 217–131, 1998.
- [3] O. J. Aldraihem, and K. A. Ahmed, "Smart beams with extension and thickness-shear piezoelectric actuators," *Smart Materials and Structures*, vol. 9, no. 1, pp. 1–9, 2000.
- [4] A. K. Ahmed, and J. A. Osama, "Deflection analysis of beams with extension and shear piezoelectric patches using discontinuity functions" *Smart Materials and Structures*, vol. 10, no. 1, pp. 212–220, 2001.
- [5] L. E. Azulay, and H. Abramovich, "Piezoelectric actuation and sensing mechanisms-Closed form solutions," *Composite Structures J.*, vol. 64, pp. 443–453, 2004.
- [6] T. Baily, and J. E. Hubbard Jr., "Distributed piezoelectric polymer active vibration control of a cantilever beam," *J. of Guidance, Control and Dynamics*, vol. 8, no.5, pp. 605–611, 1985.
- [7] A. Benjeddou, M. A. Trindade, and R. Ohayon, "New shear actuated smart structure beam finite element," *AIAA J.*, vol. 37, pp. 378–383, 1999.
- [8] E. F. Crawley, and J. De Luis, "Use of piezoelectric actuators as elements of intelligent structures," *AIAA J.*, vol. 25, pp. 1373–1385, 1987.
- [9] K. Chandrashekhara, and S. Varadarajan, "Adaptive shape control of composite beams with piezoelectric actuators," *J. of Intelligent Materials Systems and Structures*, vol. 8, pp. 112–124, 1997.
- [10] B. Culshaw, "Smart Structures : A concept or a reality," *J. of Systems and Control Engg.*, vol. 26, no. 206, pp. 1–8, 1992.
- [11] C. R. Cooper, "Shear coefficient in Timoshenko beam theory," *ASME J. of Applied Mechanics*, vol. 33, pp. 335–340, 1966.
- [12] S. B. Choi, C. Cheong, and S. Kini, "Control of flexible structures by distributed piezo-film actuators and sensors," *J. of Intelligent Materials and Structures*, vol. 16, pp. 430–435, 1995.
- [13] A. B. Chammas, and C. T. Leondes, "Pole placement by piecewise constant output feedback," *Int. J. Contr.*, vol. 29, pp. 31–38, 1979.
- [14] A. B. Chammas, and C. T. Leondes, "On the design of LTI systems by periodic output feedback, Part-I. Discrete Time pole assignment," *Int. J. Ctrl.*, vol. 27, pp. 885–894, 1978.
- [15] Chammas, A. B. and C. T. Leondes, "On the design of LTI systems by periodic output feedback, Part-II, Output feedback controllability," *Int. J. Ctrl.*, vol. 27, pp. 895–903, 1978.
- [16] C. Doschner, and M. Enzmann, "On model based controller design for smart structure," *Smart Mechanical Systems Adaptronics SAE International USA*, pp. 157–166, 1998.
- [17] P. Donthireddy, and K. Chandrashekhara, "Modeling and shape control of composite beam with embedded piezoelectric actuators," *Comp. Structures*, vol. 35, no. 2, pp. 237–244, 1996.
- [18] J. L. Fanson, and T. K. Caughey, "Positive position feedback control for structures," *AIAA J.*, vol. 18, no. 4, pp. 717–723, 1990.
- [19] J. C. Geromel, C. C. De Souza, and R. E. Skeleton, "LMI Numerical solution for output feedback stabilization," *Proc. American Contr. Conf.*, pp. 40–44, 1994.
- [20] P. Gahnet, A. Nemirovski, A. J. Laub, and M. Chilali, "LMI Tool box for Matlab", *The Math works Inc., Natick MA*, 1995.
- [21] S. Hanagud, M. W. Obal, and A. J. Callise, "Optimal vibration control by the use of piezoceramic sensors and actuators," *J. of Guidance, Control and Dyn.*, vol. 15, no. 5, pp. 1199–1206, 1992.

- [22] W. Hwang, and H. C. Park, "Finite element modeling of piezoelectric sensors and actuators", *AIAA J.*, vol. 31, no. 5, pp. 930–937, 1993.
- [23] J. B. Kosmatka, and Z. Friedman, "An improved two-node Timoshenko beam finite element", *Computers and Struct.*, vol. 47, no. 3, pp. 473–481, 1993.
- [24] W. S. Levine, and M. Athans, "On the determination of the optimal constant output feedback gains for linear multivariable systems," *IEEE Trans. Auto. Contr.*, vol. AC-15, pp. 44–48, 1970.
- [25] T. C. Manjunath, and B. Bandyopadhyay, "Modeling and fast output sampling feedback control of a smart Timoshenko cantilever beam," *International Journal of Smart Structures and Systems*, vol. 1, no. 3, ISSN 1738-1584, pp. 283–308, Sep. 2005.
- [26] T. C. Manjunath, and B. Bandyopadhyay, "Vibration control of a smart flexible cantilever beam using periodic output feedback," *Asian Journal of Control*, vol. 6, no. 1, pp. 74 - 87, Mar. 2004.
- [27] T. C. Manjunath, and B. Bandyopadhyay, "Fault tolerant control of flexible smart structures using robust decentralized periodic output sampling feedback technique," *International Journal of Smart Mater. and Struct.*, vol. 14, no. 4, pp. 624-636, Aug. 2005.
- [28] T. C. Manjunath, and B. Bandyopadhyay, R. Gupta, and M. Umopathy, "Multivariable control of a smart structure using periodic output feedback control technique," *Proc. of the Seventh International Conference on Control, Automation, Robotics and Computer Vision, ICARCV 2002, Singapore*, Paper No. 2002P1283, pp. 1481–1486, Dec. 2-5, 2002.
- [29] Manjunath, T.C., Bandyopadhyay, B. and Janardhanan, S., "Multivariable control of a smart structure using periodic output feedback control technique," *Proc. 3rd International Conference on System Identification and Control Problems, SICPRO 2004*, Institute of Control Sciences, Moscow, Russia, Paper No. 23016, pp. 1300-1312, Jan. 28 -30, 2004.
- [30] S. Raja, G. Prathap, and P. K. Sinha, P.K., "Active vibration control of composite sandwich beams with piezoelectric extension-bending and shear actuators," *Smart Materials and Structures*, vol. 11, no. 1, pp. 63–71, 2002.
- [31] S. Rao, and M. Sunar, "Piezoelectricity and its uses in disturbance sensing and control of flexible structures : A survey," *Applied Mechanics Rev.*, vol. 47, no. 2, pp. 113–119, 1994.
- [32] C. T. Sun, and X. D. Zhang, "Use of thickness-shear mode in adaptive sandwich structures," *Smart Materials and Structures J.*, vol. 3, no. 4, pp. 202–206, 1995.
- [33] V. L. Syrmos, P. Abdallah, P. Dorato, and K. Grigoriadis, "Static output feedback : A survey," *Automatica*, vol. 33, no. 2, pp. 125–137, 1997.
- [34] P. Seshu, "Textbook of Finite Element Analysis," 1st Ed. Prentice Hall of India, New Delhi, 2004.
- [35] J. Thomas, and B. A. H. Abbas, "Finite Element Methods for dynamic analysis of Timoshenko beam," *J. of Sound and Vibration*, vol. 41, pp. 291–299, 1975.
- [36] M. Umopathy, and B. Bandyopadhyay, "Control of flexible beam through smart structure concept using periodic output feedback," *System Science Journal*, vol. 26, no. 1, pp. 23–46, 2000.
- [37] H. Werner, and K. Furuta, "Simultaneous stabilization based on output measurements," *Kybernetika*, vol. 31, no. 4, pp. 395–411, 1995.
- [38] H. Werner, H., "Robust multivariable control of a turbo-generator by periodic output feedback," *Proc. American Contr. Conf.*, New Mexico, pp. 1979–1983, 1997.
- [39] Y. C. Yan, J. Lam, and Y. X. Sun, "Static output feedback stabilization: An LMI approach," *Automatica*, vol. 34, no. 12, pp. 1641–1645, 1998.
- [40] X. D. Zhang, and C. T. Sun, "Formulation of an adaptive sandwich beam," *Smart Mater. and Struct.*, vol. 5, no.6, pp. 814–823, 1996.
- [41] T. C. Manjunath, and B. Bandyopadhyay, "Modeling and fast output sampling feedback control of a smart Timoshenko cantilever beam", *Smart Structures and Systems*, vol. 1, no. 3, pp. 283–308, Sept. 2005.



T. C. Manjunath, born in Bangalore, Karnataka, India on Feb. 6, 1967 received the B.E. Degree in Electrical Engineering from the University of Bangalore in 1989 in First Class and M.E. in Automation and Control Engineering with specialization in Automation, Control and Robotics from the University of Gujarat in 1995 in First Class with Distinction, respectively. He has got a teaching experience of 17 long years in various engineering colleges all over the country and is currently working as a Research Engineer in the department of systems and control engineering, Indian Institute of Technology Bombay, India and simultaneously doing his Ph.D. in the Interdisciplinary Programme in Systems and Control Engineering, Indian Institute of Technology Bombay, Powai, Mumbai-400076, India, in the field of modeling, simulation, control and implementation of smart flexible structures using DSpace and its applications. He has published 64 papers in the various national and international journals and conferences and published two textbooks on Robotics, one of which has gone upto the third edition and the other, which has gone upto the fourth edition along with the CD. He is a student member of IEEE since 2002, SPIE student member and IOP student member since 2004, life member of ISSS and a life member of the ISTE, India. His biography was published in 23rd edition of Marquis' Who's Who in the World in 2006 issue. He has also guided more than 2 dozen robotic projects. His current research interests are in the area of Robotics, Smart Structures, Control systems, Network theory, Mechatronics, Process Control and Instrumentation, CT and DT signals and systems, Signal processing, Periodic output feedback control, Fast output feedback control, Sliding mode control of SISO and multivariable systems and its applications.



B. Bandyopadhyay, born in Birbhum village, West Bengal, India, in 1956 received his Bachelor's degree in Electronics and Communication Engineering from the University of Calcutta, Calcutta, India, and Ph.D. in Electrical Engineering from the Indian Institute of Technology, Delhi, India in 1978 and 1986, respectively. In 1987, he joined the Interdisciplinary Programme in Systems and Control Engineering, Indian Institute of Technology Bombay, India, as a faculty member,

where he is currently a Professor and the Convener. He visited the Center for System Engineering and Applied Mechanics, Universite Catholique de Louvain, Louvain-la-Neuve, Belgium, in 1993. In 1996, he was with the Lehrstuhl für Elektrische Steuerung und Regelung, Ruhr Universität Bochum, Bochum, Germany, as an Alexander von Humboldt Fellow. He revisited the Control Engineering Laboratory of Ruhr University of Bochum during May-July 2000. He has authored and coauthored 7 books and book chapters, 51 national and international journal papers and 123 conference papers, totaling to 181 publications. His research interests include the areas of large-scale systems, model reduction, reactor control, smart structures, periodic output feedback control, fast output feedback control and sliding mode control. Prof. Bandyopadhyay served as Co-Chairman of the International Organization Committee and as Chairman of the Local Arrangements Committee for the IEEE International Conference in Industrial Technology, held in Goa, India, in Jan. 2000. His biography was published in Marquis' Who's Who in the World in 1997. Prof. B. Bandyopadhyay has been nominated as one of the General Chairmen of IEEE ICIT conference to be held in Mumbai, India in December 2006.